Anomalous permittivity and plasmon resonances of copper nanoparticle conformal coatings on optical fibers

Li-Yang Shao,[1,*] Jason P. Coyle,[2] Seán T. Barry,[2] and Jacques Albert[1]

[1]*Department of Electronics, Carleton University, Ottawa, Ontario, K1S 5B6, Canada*
[2]*Department of Chemistry, Carleton University, Ottawa, Ontario, K1S 5B6, Canada*
**liyangshao@gmail.com*

Abstract: The conformal coating of a 50 nm-thick layer of copper nanoparticles deposited with pulse chemical vapor deposition of a copper (I) guanidinate precursor on the cladding of a single mode optical fiber was monitored by using a tilted fiber Bragg grating (TFBG) photo-inscribed in the fiber core. The pulse-per-pulse growth of the copper nanoparticles is readily obtained from the position and amplitudes of resonances in the reflection spectrum of the grating. In particular, we confirm that the real part of the effective complex permittivity of the deposited nano-structured copper layer is an order of magnitude larger than that of a bulk copper film at an optical wavelength of 1550 nm. We further observe a transition in the growth behavior from granular to continuous film (as determined from the complex material permittivity) after approximately 20 pulses (corresponding to an effective thickness of 25 nm). Finally, despite the remaining granularity of the film, the final copper-coated optical fiber is shown to support plasmon waves suitable for sensing, even after the growth of a thin oxide layer on the copper surface.

OCIS codes: (160.3900) Metals; (160.4236) Nanomaterials; (240.6680) Surface plasmons; (060.2370) Fiber optics sensors; (060.3735) Fiber Bragg gratings.

References and links

1. R. Rosenberg, D. C. Edelstein, C.-K. Hu, and K. P. Rodbell, "Copper metallization for high performance silicon technology," Annu. Rev. Mater. Sci. **30**(1), 229–262 (2000).
2. G. H. Chan, J. Zhao, E. M. Hicks, G. C. Schatz, and R. P. Van Duyne, "Plasmonic properties of copper nanoparticles fabricated by nanosphere lithography," Nano Lett. **7**(7), 1947–1952 (2007).
3. K. Zawada and J. Bukowska, "Surface-enhanced Raman spectroscopy studies of phenylpyridines interacting with a copper electrode surface," Surf. Sci. **507–510**(1-3), 34–39 (2002).
4. R. C. Jorgenson and S. S. Yee, "A fiber-optic chemical sensor based on surface plasmon resonance," Sens. Actuators B Chem. **12**(3), 213–220 (1993).
5. J. Homola, "Surface plasmon resonance sensors for detection of chemical and biological species," Chem. Rev. **108**(2), 462–493 (2008).
6. J. P. Coyle, W. H. Monillas, G. P. A. Yap, and S. T. Barry, "Synthesis and thermal chemistry of copper (I) guanidinates," Inorg. Chem. **47**(2), 683–689 (2008).
7. A. L. Brazeau and S. T. Barry, "Atomic layer deposition of aluminum oxide thin films from a heteroleptic, amidinate-containing precursor," Chem. Mater. **20**(23), 7287–7291 (2008).
8. N. V. Gelfond, P. P. Semyannikov, S. V. Trubin, N. B. Morozova, and I. K. Igumenov, "Deposition of Ir nanostructured thin films by pulse CVD," ECS Trans. **25**, 871–874 (2009).
9. S.-H. Kim, E.-S. Hwang, S.-Y. Han, S.-H. Pyi, N. Kawk, H. Sohn, J. Kim, and G. B. Choi, "Pulsed CVD of tungsten thin film as a nucleation layer for tungsten plug-fill," Electrochem. Solid-State Lett. **7**(9), G195–G197 (2004).
10. C.-F. Chan, C. Chen, A. Jafari, A. Laronche, D. J. Thomson, and J. Albert, "Optical fiber refractometer using narrowband cladding-mode resonance shifts," Appl. Opt. **46**(7), 1142–1149 (2007).
11. M. A. Ordal, L. L. Long, R. J. Bell, S. E. Bell, R. R. Bell, R. W. Alexander, Jr., and C. A. Ward, "Optical properties of the metals Al, Co, Cu, Au, Fe, Pb, Ni, Pd, Pt, Ag, Ti, and W in the infrared and far infrared," Appl. Opt. **22**(7), 1099–20 (1983).
12. M. Chen and R. G. Horn, "Refractive index of sparse layers of adsorbed gold nanoparticles," J. Colloid Interface Sci. **315**(2), 814–817 (2007).

#144032 - $15.00 USD Received 14 Mar 2011; revised 21 Apr 2011; accepted 21 Apr 2011; published 27 Apr 2011

13. L.-Y. Shao, Y. Shevchenko, and J. Albert, "Intrinsic temperature sensitivity of tilted fiber Bragg grating based surface plasmon resonance sensors," Opt. Express **18**(11), 11464–11471 (2010), http://www.opticsinfobase.org/abstract.cfm?URI=oe-18-11-11464.
14. J. P. Coyle, P. A. Johnson, G. A. DiLabio, S. T. Barry, and J. Müller, "Gas-phase thermolysis of a guanidinate precursor of copper studied by matrix isolation, time-of-flight mass spectrometry, and computational chemistry," Inorg. Chem. **49**(6), 2844–2850 (2010).
15. Y. Shevchenko, C. Chen, M. A. Dakka, and J. Albert, "Polarization-selective grating excitation of plasmons in cylindrical optical fibers," Opt. Lett. **35**(5), 637–639 (2010).
16. C. Chen, P. Berini, D. Feng, S. Tanev, and V. Tzolov, "Efficient and accurate numerical analysis of multilayer planar optical waveguides in lossy anisotropic media," Opt. Express **7**(8), 260–272 (2000), http://www.opticsinfobase.org/abstract.cfm?URI=oe-7-8-260.
17. T. Erdogan, "Fiber grating spectra," J. Lightwave Technol. **15**(8), 1277–1294 (1997).
18. C. Caucheteur, Y. Shevchenko, L.-Y. Shao, M. Wuilpart, and J. Albert, "High resolution interrogation of tilted fiber grating SPR sensors from polarization properties measurement," Opt. Express **19**(2), 1656–1664 (2011), http://www.opticsinfobase.org/oe/abstract.cfm?URI=oe-19-2-1656.
19. H. Du, S. W. Lee, J. Gong, C. Sun, and L. S. Wen, "Size effect of nano-copper films on complex optical constant and permittivity in infrared region," Mater. Lett. **58**(6), 1117–1120 (2004).

1. Introduction

Copper is the most widely used noble metal and it is gradually replacing aluminum as the interconnect metal in microelectronics due to its high conductivity and excellent electromigration properties [1]. Also, copper nanostructures are promising platforms for highly sensitive optical nanosensors, photonic components and surface enhanced spectroscopy because of the large surface area of metal nanoparticle aggregates and of the catalytic properties of copper [2,3]. Therefore, increasing attention is devoted to the deposition of nanoscale copper layers on miniature devices. In this paper we investigate the formation and properties of very thin conformal copper layers on the cladding of standard optical fibers. Such metal coatings (sputtered gold in particular) have been shown to support surface plasmon resonances (SPR) suitable for high resolution bio-chemical sensing [4,5]. We show here that chemical vapour deposited copper coatings that are highly granular at the nanometer scale but very smooth on the scale of the wavelength of the light propagating in the fiber can also be used for SPR sensing.

One of the best techniques for depositing thin material layers is atomic layer deposition (ALD) because of its capacity to make highly conformal thin films with precise thickness control and high aspect ratio. In a typical process, ALD involves exposing a substrate to alternating pulses of precursor vapour and a reactant gas, while inert gas purges (with nitrogen for instance) separate each exposure. In such a fashion, a sub-monolayer growth of the target film is achieved with each cycle. When the surface chemistry is such that more than a single monolayer of material is obtained, the overall process is often referred to as pulsed CVD (P-CVD). Besides copper metal films [6], ALD/P-CVD processes have been demonstrated to make aluminum oxide thin films [7], nanostructured thin iridium films [8], and tungsten thin films as a nucleation layer for tungsten plug-fill [9]. Despite the fact that film conformality is a primary property of P-CVD, there is no direct technique for real-time thickness measurements during deposition on surfaces with a very small (1-100 μm) radius of curvature. The normal thin film characterization techniques, such as ellipsometry, atomic force microscopy (AFM), scanning electron microscopy (SEM), or X-ray photoelectron spectroscopy (XPS), which are widely used for characterizing the nanoscale films on planar surfaces cannot be used on non-planar surfaces (like optical fibers). Of course this problem is compounded by the fact that P-CVD occurs inside sealed process chambers where in situ measurement is intrinsically difficult.

In this work, we demonstrate a novel method that uses a reflective TFBG sensor (see the schematic diagram in Fig. 1(a)) placed inside a P-CVD chamber for *in situ* monitoring of the growth of copper nanolayers [10]. We find that the wavelength and amplitude of certain cladding mode resonances in the reflection spectrum of the TFBG vary monotonically with the growth of copper nanoparticles on the fiber. These findings are supported by post-deposition surface morphology studies of the copper films by SEM (for the particle shapes and distributions) and AFM (for thickness measurements). An added benefit of the TFBG

#144032 - $15.00 USD Received 14 Mar 2011; revised 21 Apr 2011; accepted 21 Apr 2011; published 27 Apr 2011

measurement is that it also provides a way to measure an effective value for the complex refractive index of the layer of copper nanoparticles. As shown below, we find the values of the real part of the refractive index of the layer in the range of 3.2 to 4.8, which is five to ten times larger than the value for bulk copper at these wavelengths [11]. This anomalous behavior is in accordance with previous studies on metal nanoparticles of similar sizes [12]. Finally, we observe a clear transition in the growth curves observed with the TFBG after approximately 20 pulses and discuss the possible origins of this transition.

2. Principle and sensor fabrication

The mechanism by which the TFBG senses events occurring on the surface of the fiber cladding can be explained briefly as follows (more details can be found in [10]). A TFBG inscribed in the core of an optical fiber couples light from the core to a large number of cladding modes, but each coupling occurs at a very specific wavelength over a wide spectral range. The Bragg wavelength and cladding mode resonance wavelengths λ_{Bragg} and λ_{clad}^{i} of TFBG are determined by the following phase matching condition [10]:

$$\lambda_{Bragg} = N_{eff}(core) * \Lambda / \cos(\theta) \quad (1.a)$$

$$\lambda_{clad}^{i} = (N_{eff}(core) + N_{eff}^{i}(clad)) * \Lambda / \cos(\theta) \quad (1.b)$$

where Λ is the grating period, θ the tilt angle of the grating planes, $N_{eff}(core)$ and $N_{eff}^{i}(clad)$ are the effective refractive index of the core mode and i th order cladding mode measured at the resonance wavelengths. When the TFBG is exposed to a perturbation (here, nanoparticles of copper deposited on the cladding surface), the effective index of each cladding mode $N_{eff}^{i}(clad)$ is modified by the change in the refractive index (RI) of its immediate environment (but not the core mode effective index). As a consequence of Eq. (1.b), the resonance wavelengths of cladding modes shift in response to the external RI changes. Since the RI of metals is complex, an additional effect comes into play as the effective index of the cladding modes also becomes complex (i.e. the modes becomes lossy) and the amplitude of the resonance also changes significantly as a result.

For these experiments we fabricated 1-cm-long TFBGs with a tilt angle of 10° in hydrogen-loaded Corning SMF-28 fibers using a pulsed KrF excimer laser and the phase mask technique [13]. The fiber was soaked in a hydrogen chamber for 12 days at 2500 psi and room temperature (25°C) to improve its photosensitivity and allow the formation of a strong grating. The period of the phase mask was 1106.5nm, which led to a TFBG Bragg wavelength of 1602nm (the wavelength at which core mode back reflects upon itself). Taking into account the limited space inside the CVD chamber and to avoid having to thread the fiber in and out of the chamber, we cleaved the fiber 2 cm downstream from the TFBG and coated it with a gold mirror in order to have the core guided light reflect from the end and come back upon itself (thereby going through the grating twice). The reflection of the TFBG sensor was measured by an optical sensing analyzer (Si720, from Micron Optics) with a polarization controller (JDS Uniphase) in the beam path. The polarization controller is used to align the linear polarization of the light incident on the grating along specific directions relative to the plane of the grating tilt (for reasons to be explained below). The wavelength resolution in the measurement is 0.0025nm at a scan rate of 1.2 seconds per full spectrum range (the high speed scanning rate is important for "real time" measurement in the current experiment). Figure 1(b) shows the reflection spectrum of a 10° TFBG with a gold mirror before deposition, where the inset is a photo of the fabricated TFBG sensor. The cladding mode resonances to be used for sensing events on the cladding surface are those located on the short wavelength side of the spectrum, because their evanescent field extends relatively further outside of the cladding (a few microns in fact). On the other hand, the core mode Bragg

#144032 - $15.00 USD Received 14 Mar 2011; revised 21 Apr 2011; accepted 21 Apr 2011; published 27 Apr 2011

resonance near 1602 nm is totally immune to the surrounding RI changes and can be used as temperature and optical power level reference [10].

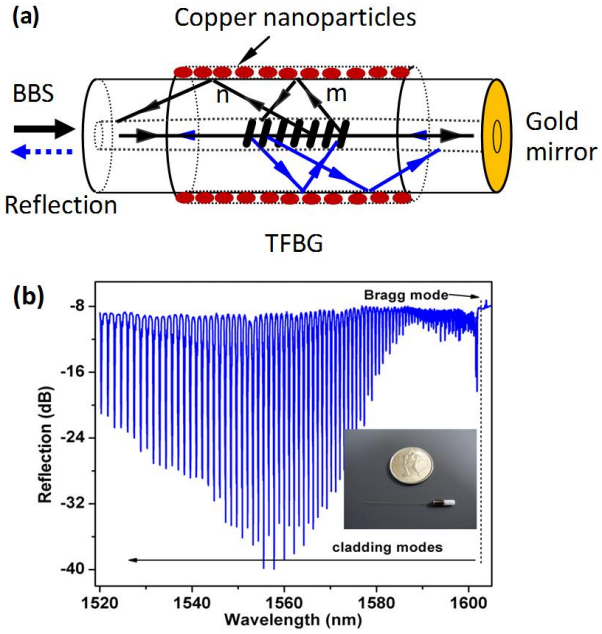

Fig. 1. (a) Schematic diagram of TFBG sensor with a gold mirror; (b) Reflection spectrum of 10° TFBG sensor before copper deposition, where the inset shows the photo of fabricated TFBG sensor (in the fiber sticking out of on the left of the black and white connector).

3. P-CVD deposition of Cu nanoparticles

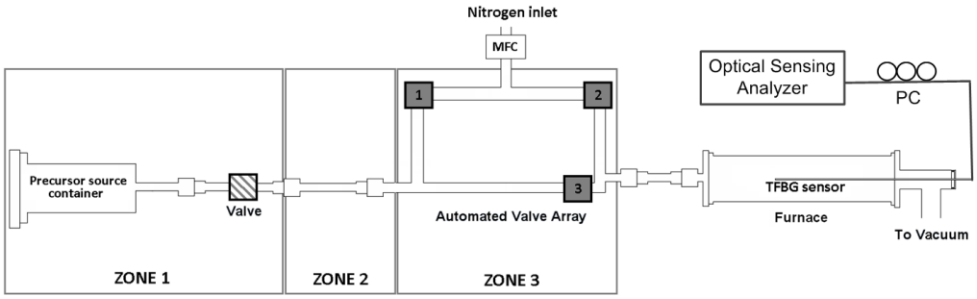

Fig. 2. Schematic diagram of the pulsed CVD reactor and optical measurement setup (PC: polarization controller)

The deposition apparatus used for pulsed CVD was a home-made hot walled reactor using an automated valve array comprised of three pneumatic valves (Fig. 2). All tubing was made from 316 stainless steel and 1/4" VCR or 2 ¾" CF fittings were used throughout on the upstream side of the furnace. Vacuum tubing and the TFBG sensor adaptor were connected using Viton o-rings in 25 KF flanges. The TFBG sensor adaptor was constructed from an end cap with a small hole drilled through where the fiber was inserted and fixed with epoxy. The length of the fiber was sufficient place the TFBGs in the centre of the reactor. The valve array was heated to 145 °C (Zone 3) and the inter-tubing between the source container and valve array was heated to 135 °C (Zone 2) to avoid condensation of the precursor before reaching the deposition chamber. The deposition chamber with its TFBG sensor was a stainless steel

#144032 - $15.00 USD Received 14 Mar 2011; revised 21 Apr 2011; accepted 21 Apr 2011; published 27 Apr 2011

tube with a diameter of one inch surrounded by a tube furnace which was heated to 200 °C. The precursor source container was heated to 125 °C (Zone 1), and was connected to the apparatus by a manual valve. Before the deposition, the reactor was evacuated to less than 60 mTorr. Copper film growth on the TFBG sensor was controlled by limiting the flow of Cu precursor using pulsed CVD. The vaporous precursor obtained by heating under vacuum could be pulsed into the furnace in a controlled manner. The length of time of each pulse and the time separating each pulse were kept constant to ensure that the amount of precursor vapour introduced into the furnace each deposition cycle was consistent. Nitrogen was used as a carrier and purging gas and was introduced by a mass flow controller (MFC) set to 150 sccm. The pulsing cycle for a typical CVD experiment was (1) 5.0 s purge of furnace with N_2, (2) evacuate furnace and fill source container with N_2 for 3.0 s; (3) expel vapor in source container to furnace for 2.0 s; (4) 3.0 s purge of furnace with N_2; (5) allow evacuation of furnace for 2.0 s. This pulsing cycle was typically repeated 10-40 times during one deposition. The gaseous precursor deposits metallic copper by a single-source thermal decomposition mechanism on all surfaces of the deposition chamber, including the surface of the optical fiber, for furnace temperatures above 160 °C. Previous work identified the thermal decomposition mechanism as β-hydride elimination (Fig. 3) [14]. The copper (I) guanidinate employed in this work has sufficient vapor pressure at temperatures lower than its onset of thermal decomposition to be a suitable pulsed CVD precursor.

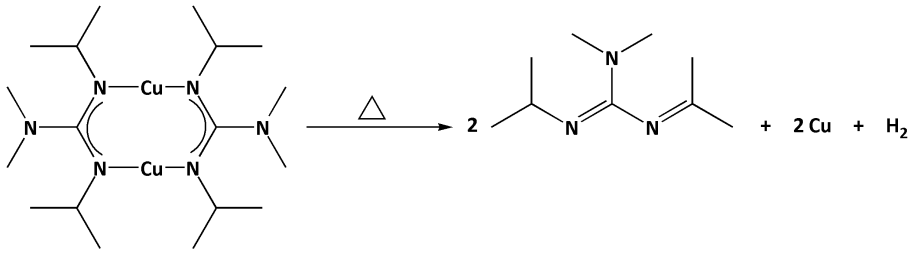

Fig. 3. Gas phase thermolysis of the copper(I) guanidinate pulsed CVD precursor.

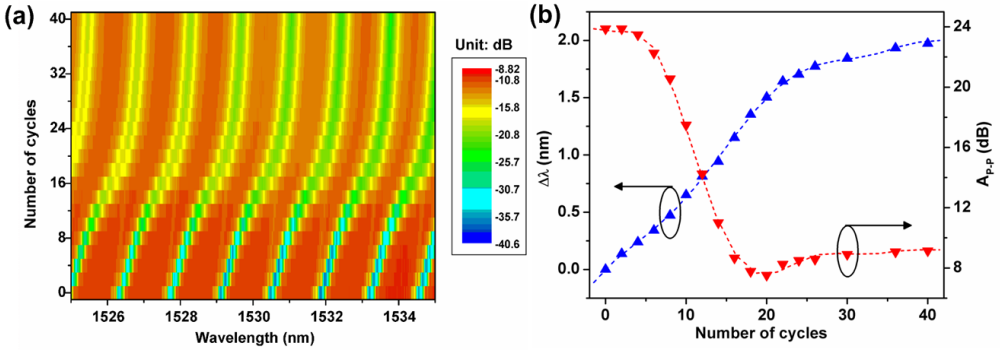

Fig. 4. (a) Spectral evolution of TFBG at P-polarization state (Colour indicates resonance amplitude) and (b) corresponding wavelength and peak-to-peak amplitude changes of one cladding mode resonance around 1526.2 nm as a function of the number of cycles.

Previous experiments with uniform metal coatings deposited using sputtering had determined that the sensor's response is dependent on the polarization state of incident light [15]. When the input core mode light polarization is aligned along the tilt plane of the grating (P-polarization) the light coupled to high order cladding modes is polarized predominantly in the radial direction at the cladding boundary and thus able to excite plasmon resonances in uniform metal coatings. No plasmon resonances are observed for S-polarized input light. The spectra of the TFBG sensor were recorded every 2 cycles for P- and S-polarization states. It is clear that for the deposition of nanoparticles of copper, resonances associated with P-polarized

#144032 - $15.00 USD Received 14 Mar 2011; revised 21 Apr 2011; accepted 21 Apr 2011; published 27 Apr 2011

light react much more strongly that those associated with S-polarized light. Here we only show the evolution of the spectra at P-polarization as a function of the number of cycles during the pulsed CVD copper deposition experiment in Fig. 4(a). Figure 4(b) plots the corresponding wavelength and amplitude (peak-to-peak) changes of one cladding mode resonance around 1526.2 nm for P-polarization.

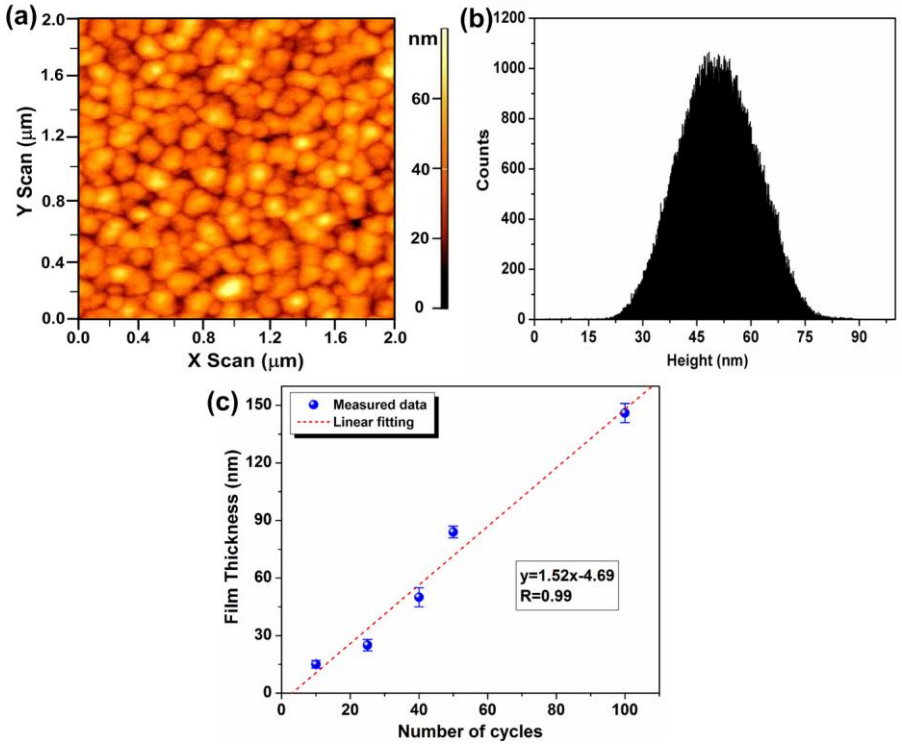

Fig. 5. AFM image (a) and bearing histogram (b) of Cu film on flat substrate after deposition of 40 pulsing cycles. The measured average thickness is 50 nm. (c) Absolute AFM height measurements on flat substrates up to 100 pulsing cycles.

An AFM scan of the flat substrate was performed in semi-contact mode and the results are shown in Fig. 5(a), along with the bearing histogram of the AFM measurement in Fig. 5(b). Using this, along with absolute AFM height measurements on a flat substrate, with the film partially removed, we estimate the thickness of the deposited Cu film to have an average of 50 nm with a deviation of ± 5nm. These experiments were run several times up to 100 pulsing cycles and we found that for these conditions the growth of Cu nanolayer is quasi-linear with a slope rate of 1.52 nm/cycle (Fig. 5(c)). Simultaneous measurements of TFBG resonances yielded total resonant wavelength shifts of 2.0 nm after 40 cycles, while the peak-to-peak amplitude decrease was 16 dB. However both TFBG parameters did not show a linear response over the full deposition process. In fact both the wavelength shift and peak-to-peak amplitude evolve in quasi-linear fashion for the first 20 cycles and then saturate. Over the linear portion of the TFBG parameter evolution, the sensitivities of the TFBG sensor were obtained as 80 pm/cycle in wavelength and −0.78 dB/cycle in amplitude corresponding to 53 pm/nm(Cu) and −0.52 dB/nm(Cu). These sensitivities are significant considering that the resonances used have typical full widths at half maximum of the order of 100 pm and since measuring instruments can easily achieve 0.1 dB power level accuracy (especially for relative power and wavelength measurements that use the core mode reflection as a reference for both parameters). This makes the measurements of nanometer-scale thickness changes very easy to carry out.

#144032 - $15.00 USD Received 14 Mar 2011; revised 21 Apr 2011; accepted 21 Apr 2011; published 27 Apr 2011

4. Analysis and discussion

In addition to thickness monitoring, further investigation in the response of the TFBG resonances can provide information about changes in the real and imaginary parts of the effective index of the cladding mode that is coupled by the grating and by extension about the optical properties of the deposited layers during the deposition process.

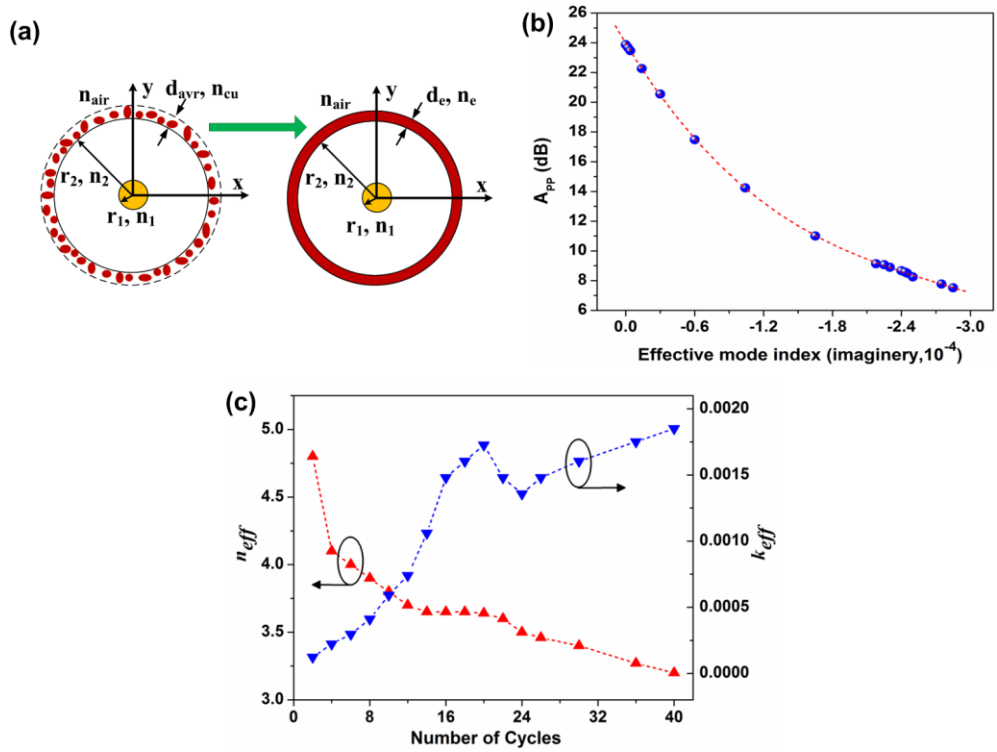

Fig. 6. (a) Cross-section of the four layer model of the fiber with sparse layer of copper nanoparticles (left) and an equivalent copper coating (right). (b) Calculation of the change in peak to peak resonance amplitude vs the imaginary part of the effective index of the cladding mode; (c) Resulting effective complex refractive index of copper nanoparticles on the cladding of the fiber vs pulsing cycles.

In order to do this, for each cycle of deposition we approximate the layer of deposited nanoparticles by an equivalent uniform coating of the same thickness. We then use fiber grating simulation software to calculate which value of complex permittivity of the uniform layer results in the observed shifts of the resonance amplitude and wavelength (the two measured parameters fully determine the two unknowns, i.e. the real and imaginary part of the film permittivity). We use a commercially available complex fiber mode solver (FIMMWAVE, by Photon Design) to calculate the effect of these layers on the mode in question. The structure we modeled is an optical fiber coated with a uniform layer of thickness of d_{avr} (obtained for each cycle by the calibration factor between cycle number and thickness given above), an effective complex refractive index ($n_{eff} - jk_{eff}$) to be determined, and air (index of refraction = 1) in the surrounding environment (see Fig. 6(a)). The parameters of the fiber (a standard telecommunication fiber) were as follows: the radii of fiber core and cladding, r_1 = 4.15 μm and r_2 = 62.5 μm; $d_e = d_{avr}$, where d_e is the thickness of equivalent copper nanolayer ranging from 0 to 50 nm; the corresponding refractive indices were n_1 = 1.450, n_2 = 1.444 and n_{air} = 1.0 [16]. The mode solver reveals that prior to deposition (d_e = 0), the effective index of the mode used for Fig. 4(b) is real and equal to 1.3094. Also prior to deposition, the amplitude of the resonance can be used to calculate the

#144032 - $15.00 USD Received 14 Mar 2011; revised 21 Apr 2011; accepted 21 Apr 2011; published 27 Apr 2011

coupling coefficient of the grating for this mode, using another commercial simulation tool based on coupled mode theory (OptiGrating, from OptiWave Inc.). The coupling coefficient value is 3.44 cm^{-1} for the case described here [17]. We now use a perturbation approach and assume that the change in the resonance amplitude is mainly due to the increase in loss experienced by the cladding mode when the lossy copper nanoparticles deposit on the cladding (rather than to a change in mode field amplitude near the core of the fiber, which would also lead to a change in the coupling coefficient). Using OptiGrating again allows us to plot a template for the change in peak to peak resonance amplitude vs the imaginary part of the effective index of the cladding mode (shown in Fig. 6(b) for the particular resonance used here).

Therefore, each measurement provides a new value of the real and imaginary parts of the cladding mode effective index and consequently, through iterations with the mode solver at the corresponding thickness, new values for the effective complex permittivity of the deposited film (expressed in terms of complex refractive index: n_{eff} and k_{eff}). Figure 6(c) shows the result of this calculation for the experimental data of Fig. 4(b) as a function of the number of pulsing cycles. Compared to the value for bulk copper at these wavelengths (0.58-8i) [11], the effective real part of the refractive index of the deposited copper nanoparticles layer is much larger (decreasing from 4.8 to 3.2 as the layer grows). This anomalous result was actually observed previously for sparse layers of spherical metallic nanoparticles deposited on planar substrates and was tentatively explained by a Maxwell-Garnett model for the effective refractive index of aggregate materials [12]. Similarly, the imaginary part of the effective refractive index of the layer is orders of magnitude smaller than for the bulk (but this is expected for aggregates of sub-wavelength nanoparticles surrounded by air).

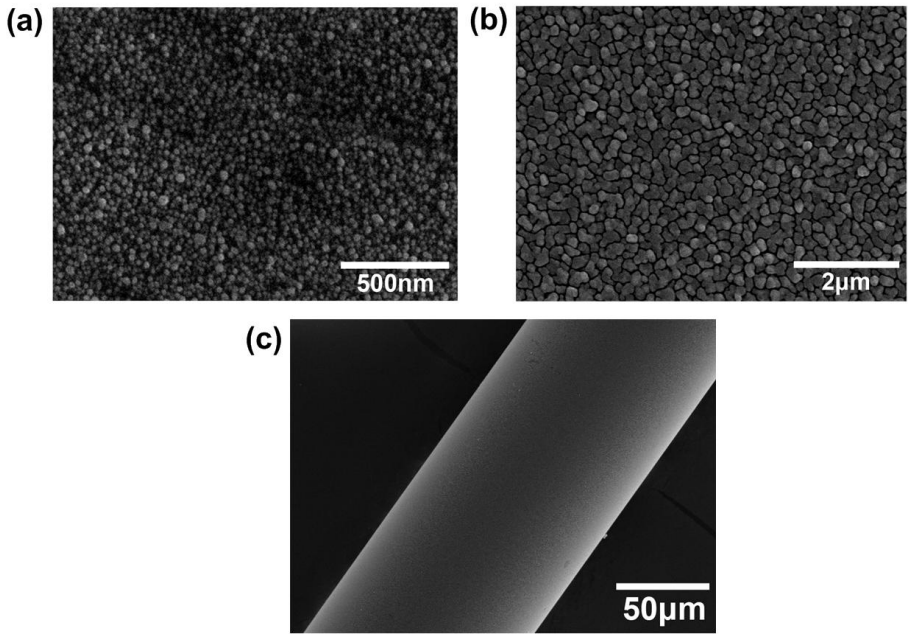

Fig. 7. SEM images of Cu nanoparticles deposited on the fiber surface of (a) 10 cycles, (b) 40 cycles and (c) whole fiber at 40 cycles.

The last feature of interest that we discuss is the discontinuity in both amplitude and wavelength shift observed near 20 pulses. In order to try to understand why this occurs we made experiments with fewer pulses to measure surface morphologies (by SEM) on both sides of the transition. Figures 7(a) and 7(b) shows the SEM images of Cu nanoparticles deposited on the fiber surface after 10 cycles and 40 cycles, respectively. The Cu film after 10 cycles is made up of a relatively sparse layer of individual particles ranging in sizes from a few nm to

#144032 - $15.00 USD Received 14 Mar 2011; revised 21 Apr 2011; accepted 21 Apr 2011; published 27 Apr 2011

about 50 nm, while the image of the film after 40 cycles shows particle aggregates that have large (200 nm and more) lateral extent and conforming boundaries (remember that the average thickness after 40 cycles is only 50 nm). So the particles aggregate into thin plates instead of growing in all directions. From these observations, we speculate at the moment that the discontinuity observed at 20 cycles corresponds to a sparse to semi-continuous film transition where the particles begin to touch each other and amalgamate laterally. Any further discussion of the effect of this transition on the results of Fig. 6 is beyond the scope of the present paper and will require more experimental and theoretical investigations. Finally, it is worth noting that on the scale of the wavelength of the light propagating in the fiber (1550 nm), and even more so on the scale of the fiber dimensions itself (125 μm diameter), Fig. 7(c) shows that the deposited films are very smooth and regular.

5. Surface plasmon resonances of Cu nanoparticles

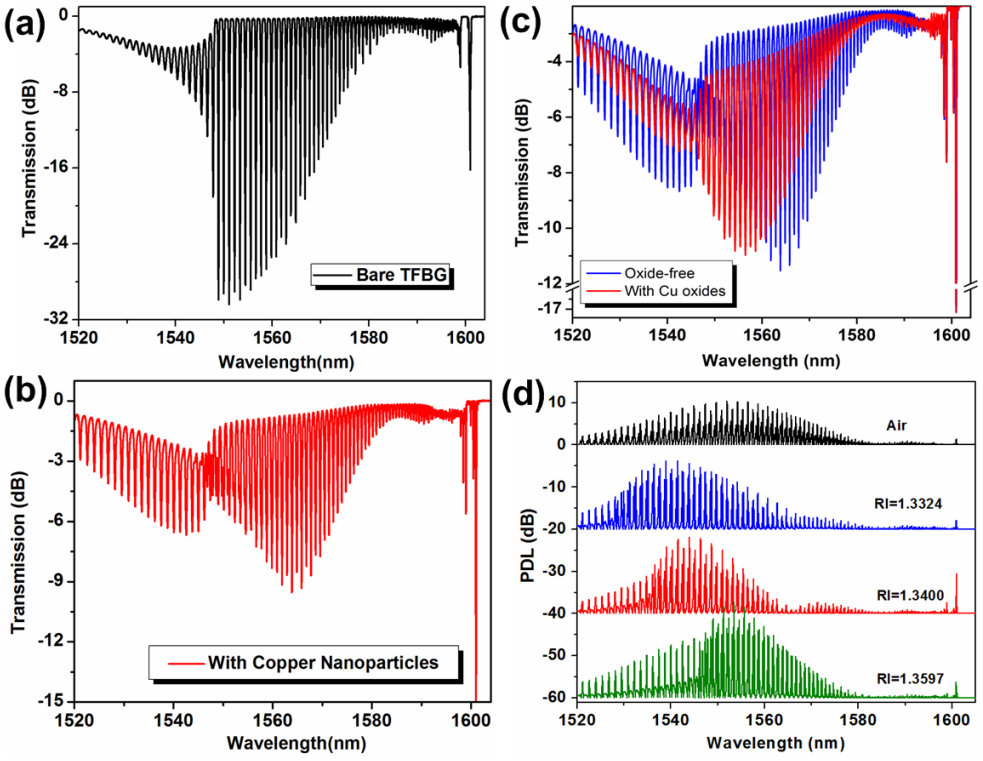

Fig. 8. Transmission spectra of (a) bare TFBG and (b) Cu nanoparticles coated TFBG in the solution (RI = 1.3597); (c)comparison spectra of the TFBGs with oxide-free Cu nanoparticles and Cu oxides; (d) PDL spectra evolution of Cu nanoparticles coated TFBG in air and three liquids

We also found that the deposited copper coatings could support surface plasmons excited by light coupled out of the fiber core by the TFBG. Compared to gold (previously used for this purpose), copper metal is prone to surface oxidation that affects its optical properties significantly, so the plasmonic properties of copper have not received much attention as compared to silver and gold. However, studies of room temperature oxide growth on spherical copper nanoparticles indicate that the initial oxide film growth is very slow (~0.031 nm/day) [2]. In order to remove this effect from our experiments, a simple oxide removal procedure using glacial acetic acid was implemented to ensure the purity of the copper nanoparticles on the surface of TFBG sensor during SPR test (acetic acid only etches copper oxide and not copper metal). Immediately before testing and between each test solution, the copper coated

#144032 - $15.00 USD Received 14 Mar 2011; revised 21 Apr 2011; accepted 21 Apr 2011; published 27 Apr 2011

TFBG sensor was treated in acetic acid and dried by flowing nitrogen gas. SPR test consisted of inserting the sensor in three solutions with refractive indices of 1.3324, 1.3400, and 1.3597 respectively. Figures 8(a) and 8(b) show the transmission spectra of the TFBGs without/with copper nanoparticles in the solution (RI = 1.3597). The bare TFBG only experiences cladding mode cut-off (Fig. 8(a)), while the spectrum of TFBG sensor with copper nanoparticles shows a dip in the resonance amplitude associated with SPR effects (similar to the gold coated one in ref. 15). Figure 8(c) shows a comparison between the spectra of TFBG sensors with and without oxidation of the copper, showing the amount of degradation of the SPR signature. While oxidized copper-coated TFBGs are still usable for sensing, this degradation can be compensated by dipping in acidic solutions but this process cannot be repeated indefinitely as each time a fraction of the copper gets etched away as copper oxide. The last experimental result (Fig. 8(d)) shows the polarization dependent loss spectra of the coated TFBGs in air and three liquids. As presented in [18], PDL measurement is the most practical method to spectrally locate the SPR. The refractive index sensitivity of Cu coated TFBG is obtained as 585.3 nm/RIU, which is comparable to a SPR-TFBG with a sputtered gold coating [13,15].

6. Conclusion

In conclusion, a TFBG sensor has been shown to be able to detect every step of the pulsed CVD deposition of nanometer-sized copper nanoparticles conformally around the circumference of a 125 μm diameter standard optical fiber. The growth of the copper nanoparticles and the formation of a semi-continuous film are detected *in situ* and in real-time by measuring the spectral position and amplitude of one of the grating resonances. Of special interest is the unexpected observation that some of the TFBG resonances shift strongly (relative to their widths) in the very first stages of pulsed deposition when the copper particles form layers consisting of particles with very irregular shapes of approximate diameters of a few nm, about three orders of magnitude smaller than the wavelength of the light used. These measurements further allowed the calculation of the complex effective refractive index of the deposited copper nanoparticles, yielding values widely different from those of bulk copper but consistent with expected values for sparse layers of metallic nanostructures [19]. With help from SEM examinations, a transition observed in the sensor response was attributed to a change in the film morphology from granular to semi-continuous in the plane of the surface coated. This transition could then be used to control the morphology of deposited films, either on the TFBG samples themselves or on other surfaces by using the TFBGs as process monitors. In fact, these features of the TFBG (along with the other TFBG desirable features of small size, low cost, recyclability, and low cross-sensitivity to other perturbations, including temperature) make it an ideal candidate as a process monitor for ALD and P-CVD coating techniques either in research or commercial environments. Finally, the plasmonic properties of copper coated TFBG have also been investigated by inserting the sensor in liquids with different refractive indices and confirmed that the granular copper films do support plasmon-like resonances. While the oxidation of the copper hinders the quality of the resonances, the copper surfaces can be refreshed with a simple liquid based etch of the thin oxidized layer. The achieved sensitivity of 585.3 nm/RIU is comparable to gold based fiber SPR but an additional interest of Cu-based SPR-TFBGs arises because of their strong reactivity with oxygen. Therefore they can be developed to study the Cu oxididation process or in sensing applications of oxide gases (like CO_2 or NO_2).

Acknowledgments

This work is supported by the Natural Sciences and Engineering Research Council of Canada, the Canada Foundation for Innovation, the Canada Research Chairs program (J. Albert), LxDATA, and the National Natural Science Foundation of China (NSFC) under Grant No. 61007050. The authors also thank Dr. Chengkun Chen from the University of Ottawa for helpful discussion in the simulation of fiber modes.

#144032 - $15.00 USD Received 14 Mar 2011; revised 21 Apr 2011; accepted 21 Apr 2011; published 27 Apr 2011